https://doi.org/10.15407/ujpe65.10.924

E.G. GALKINA,[1] V.E. KIREEV,[2] R.V. OVCHAROV,[3] R.S. KHYMYN,[4]
B.A. IVANOV [1, 2, 3]

[1] Institute of Physics, Nat. Acad. of Sci. of Ukraine
(46, Nauky Ave., Kyiv 03028, Ukraine)
[2] Institute of Magnetism, Nat. Acad. of Sci. of Ukraine
and Ministry of Education and Science of Ukraine
(36b, Academician Vernadsky Blvd., Kyiv 03142, Ukraine; e-mail: bor.a.ivanov@gmail.com)
[3] Taras Shevchenko National University of Kyiv, Faculty of Physics
(4, Academician Glushkov Ave., Kyiv 03127, Ukraine)
[4] Department of Physics, University of Gothenburg
(41296 Gothenburg, Sweden)

SPIN DYNAMICS IN ANTIFERROMAGNETS WITH DOMAIN WALLS AND DISCLINATIONS

The spin dynamics in antiferromagnets with atomic dislocations and dislocation-induced spin disclinations has been discussed. It is shown how the usual sigma-model equation can be used to describe it. The dynamical states with the spatially inhomogeneous spin precession are studied. It is demonstrated that such an internal dynamics of the spin disclinations and the related domain walls can serve as a basis for creating a spin-Hall nanogenerator pumped with a spin current and characterized by a low excitation threshold.

K e y w o r d s: antiferromagnet, disclination, spin current.

1. Introduction and Formulation of the Problem

The study of antiferromagnets (AFMs) began in the 1930s, shortly after a consistent quantum-mechanical theory of magnetic ordering driven by the spin-exchange interaction had been developed. The exchange interaction between neighbor spins in AFMs have a specific feature: it makes their antiparallel orientation advantageous. In the simplest case, the crystal lattice of an AFM contains two magnetic sublattices with the magnetizations $\mathbf{M}_1$ and $\mathbf{M}_2$. Those magnetization vectors are equal in magnitude and oriented in antiparallel to each other. Therefore, the time reflection symmetry in AFMs is broken, but the total AFM magnetization equals zero, $\mathbf{M}_1 + \mathbf{M}_2 = \mathbf{M} = 0$. The magnetic ordering in the AFM is characterized by the antiferromagnetic vector $\mathbf{L} = \mathbf{M}_1 - \mathbf{M}_2$.

The studies of antiferromagnets comprise a substantial domain in the fundamental physics of magnetism. The symmetry plays an essentially important role while describing the physical properties of AFMs. By definition, the AFM sublattices are crystallographically equivalent, i.e. there is an element of the crystal symmetry group (the symmetry group of the paramagnetic phase, the "paraphase") that transforms them into each other (see the book by Turov *et al.* [1]). In other words, the crystal symmetry group of AFMs includes at least one symmetry element that transforms the magnetic sublattices into each other. In particular, this symmetry property makes the existence of a magnetization state with a strictly zero magnetization, $|\mathbf{M}| = 0$, possible, i.e. there is a possibility for the magnetizations of the sublattices to exactly compensate each other, when the external parameters (e.g., the temperature) are varied in wide intervals of their values. In this case, the total magnetization and the total spin density of the AFM simultaneously vanish.

Following Turov *et al.* [1], let us refer to the symmetry operations that interchange and do not interchange the magnetic sublattices as odd and even, respectively. A criterion for antiferromagnetism to take place is the presence of at least one odd symmetry element in the paraphase. Under the action of the odd element, the lattices "change places", $\mathbf{M}_1 \to \mathbf{M}_2$, $\mathbf{M}_2 \to \mathbf{M}_1$, and the antiferromagnetic vector $\mathbf{L}$ changes its sign. Those conditions distinguish AFMs

from ferrimagnets. The latter also have magnetic sublattices with "antiferromagnetic" exchange interaction, but those sublattices are not equivalent (see works [1–4]). For ferrimagnets, the total magnetization can also become zero, but only at a certain temperature (the compensation point). For ferrimagnets, the compensation temperatures of spin densities and sublattice magnetizations may not coincide.

AFMs are characterized by a number of interesting properties, among which the exchange enhancement of their dynamic parameters is the most important one (see reviews [1, 5–8] and the next Section). AFMs have higher magnetic resonance frequencies and higher velocities of magnons and magnetic solitons in comparison with ferromagnets, for which the values of exchange integrals and anisotropy constants are the same. In essence, those features are a result of the fact that the main dynamic variable for AFMs is the antiferromagnetic vector **L**. The dynamics of the vector **L** is described by the so-called sigma model, and the exchange enhancement can be directly explained by the presence of an odd element of the AFM symmetry group.

Of interest are the peculiar "non-magnetic" properties of AFMs: optical [1, 9–14], galvanomagnetic [1, 10], and acoustic ones [1, 10, 15]. Due to the long-term studies of the magnetic ordering in AFMs and the related "non-magnetic" phenomena, the decisive role of the character of just the odd symmetry elements has been established. Here, the most striking example is the appearance of the weak ferromagnetism in AFMs. This phenomenon becomes possible in the case where the odd symmetry elements are rotations, but it is forbidden, if they include odd translations or inversion [16, 17]. The same restrictions are also typical of the **L**-dependent (antiferromagnetic) Faraday and Hall effects associated with the **L** vector rather than the AFM magnetization [1, 10, 12]. For example, the magnetoelectric effect is possible, if the odd operation is the inversion [1, 10].

The interest in the study of static and, especially, dynamic properties of AFMs has been growing permanently. The main reason is that the spin dynamics in AFMs is faster than in ferromagnets. In particular, the spin oscillation frequencies in AFMs range from hundreds of gigahertz to several terahertz and belong to the terahertz interval. A necessity in exploiting this interval has been growing in recent years, because the corresponding frequencies are actively used in astrophysics, physics of atmosphere, biology, medicine, in security systems, the systems for detecting hazardous materials, and so forth (see the recent collective review [18]).

The application of AFMs in the terahertz technique is based on various physical effects. The application of femtosecond lasers (with a pulse duration time shorter than 100 fs) allows the non-thermal excitation of spin oscillations in transparent AFMs [19–27], which can be used to create generators of electromagnetic waves in the terahertz interval with optical pumping and a control over the radiation parameters [28–30]. The capability of such excitation is based on the effects that are inverse to the well-known magneto-optical Faraday and Cotton–Mouton effects [7, 8]. In such a way, nonlinear modes of the vector **L** motion, which correspond to the "inertial" switching of the vector **L** from one equilibrium state into another (the dynamic spin reorientation) [31, 32], can also be excited. Such a possibility opens the prospect of the ultra-fast information recording and processing [7].

Great expectations are associated with the application of AFMs in spintronics [34–38]. It was shown that the spin-current effects in AFMs can also be rather substantial [33]. AFMs can effectively conduct the spin current and even the superconducting spin current [39–44]. The predicted effect of the spin current growth in the AFM [45] has been recently observed experimentally [46]. The effects of the direction switching of the vector **L** under the spin-current action [47, 48] were observed. The resonant spin pumping using an AFM as an active element was performed at frequencies up to 200 GHz [49] and up to 450 GHz [50].

All that, in principle, makes it possible to create a purely spintronic AFM-based nanooscillator, in which both the spin-current pumping and the desired signal readout is realized by use of the spin current (e.g., by means of the direct and inverse spin Hall effects) [51–54]. Such a generator could efficiently operate in the subterahertz and terahertz frequency ranges. Here, however, there arises a problem associated with the specific feature of the AFM dynamics. Namely, the spin current, as a rule, can only excite a purely planar rotation of the vector **L**, which does not create ac signal owing to the spin Hall effect. Note that, in ferrimagnets which are also characterized by ultrahigh frequencies of spin oscillations, the spin preces-

sion is not planar [4, 55–57], so that the aforementioned problem does not arise. Various ways to solve this problem for AFMs were discussed in the recent publications [37,38,58–63]. But their implementation is connected with an increase of the pumping current threshold value [58] or a considerable complication of the device design [60].

The application of an AFM domain wall as an active element in the nano-oscillator has also been proposed [64]. The presence of domains and domain walls in AFMs, as well as a possibility to control them, is well known. In weak ferromagnets, regular domain structures appear following the standard mechanism of minimizing the magnetodipole energy [5,6]. But in "pure" AFMs without weak ferromagnetism, such a mechanism of the equilibrium domain structure formation does not work.

The formation of an equilibrium domain structure can be a result of the action of long-range forces belonging to another type, namely, the magnetoelastic interaction [65–69]. In the works of S.M. Ryabchenko's group, it was found that, in a lot of AFMs, the equilibrium (or close to equilibrium) multidomain AFM state can exist in a wide temperature interval ranging from helium to Néel temperature [70–72]. It was proved that an inhomogeneous, elastically deformed state of the crystal provides a minimum in the total energy of the AFM crystal. In the works by S.M. Ryabchenko and his colleagues, the role of defects was also marked; in particular, dislocations, which locally change the character of magnetic anisotropy, so that an inhomogeneous spin state becomes favorable [70–72]. Those mechanisms are universal and relatively weakly depend on the magnetic symmetry, in particular, on the parity of the crystal symmetry elements.

There are also known specific inhomogeneous AFM states that exist due to the existence of the odd elementary translation. In a sense, such AFMs are "textbook" ones. Just in them, the corresponding magnetic and atomic unit cells can be different. In particular, such AFMs include the oxides of transition metals – e.g., NiO and CoO – as well as plenty of materials with metallic conductivity – e.g., Cr, FeMn, IrMn, and Mn_2Au – which are promising for ultrafast AFM-based spintronics. The presence of the odd translation leads to the prohibition of many interesting effects such as the weak ferromagnetism and the abovementioned **L**-dependent Faraday and Hall effects. At the same time, the presence of odd translations in the AFM symmetry group is responsible for the existence of peculiarities in the properties of non-ideal crystals containing atomic dislocations and their systems. As was noted as long ago as in the 1970s, any dislocation whose Burgers vector coincides with the odd translation vector creates a macroscopic inhomogeneity (spin disclination) in the spin distribution [73,74]. An analysis of the global topological properties of the vector **L** distribution in AFMs with dislocations or vortices can be found in review [75]. An analysis of static spin states for magnets with antiferromagnetic interaction is rather complicated in this case, whereas the dynamic states, as far as we know, have not been studied yet.

In this paper, we will discuss a version of the sigma model for the vector **L** in which the presence of atomic dislocations and dislocation-generated spin disclinations in the AFM spin system is taken into account in the macroscopic approximation. The dynamic states corresponding to the spatially inhomogeneous spin precession are studied. It will be shown that such an internal dynamics of spin disclinations and related domain walls can be useful while creating a spin-Hall nanogenerator with spin-current pumping and a low excitation threshold.

2. Description of AFMs with Dislocations in the Framework of the Sigma Model

When developing the standard phenomenological theory for AFMs with a perfect lattice, the magnetization vectors of the sublattices, $\mathbf{M}_1$ and $\mathbf{M}_2$ or their combinations $\mathbf{M} = \mathbf{M}_1 + \mathbf{M}_2$ and $\mathbf{L} = \mathbf{M}_1 - \mathbf{M}_2$ are considered. It is convenient to introduce the normalized vectors

$$\mathbf{l} = \frac{\mathbf{M}_1 - \mathbf{M}_2}{2M_0}, \quad \mathbf{m} = \frac{\mathbf{M}_1 + \mathbf{M}_2}{2M_0}, \tag{1}$$

where M_0 is the sublattice magnetization in the AFM. Vectors (1) are constrained by the relations

$$\mathbf{l}^2 + \mathbf{m}^2 = 1, \quad \mathbf{ml} = 0. \tag{2}$$

Let there be an atomic dislocation in the crystal, and let its Burgers vector be an odd translation vector. When going around such a dislocation, the sublattices change places, i.e. $\mathbf{M}_1 \leftrightarrow \mathbf{M}_2$, and the vector $\mathbf{l}$ has to change its sign. The appearance of disclinations in the crystal with an edge dislocation can be

explained by the fact that any contour drawn along the exchange bonds and encircling the dislocation line contains an odd number of sites and does not allow a perfect antiferromagnetic ordering. A real pattern of the spin distribution over the AFM volume, including the dislocation region, can be quite complicated.

As an example, let us consider layered AFMs belonging to dihalides of the iron-group elements – $CoCl_2$, $FeCl_2$, $NiCl_2$, and $CoBr_2$ – for which the ferromagnetic interaction between two spins located in the same atomic plane (it is described by the exchange integral $J_{\rm op}$) is much stronger than the antiferromagnetic interaction between two spins located in the neighbor planes (it is described by the exchange integral $J_{\rm ip}$), i.e. $J_{\rm op} \gg J_{\rm ip}$. If such an AFM contains a screw dislocation, the atomic plane transforms into a helical surface (similar to the Riemann surface of the complex-valued function $w = \ln z$), the whole picture being far, at first glance, from the standard sublattice scheme [76]. However, a corresponding analysis showed that deviations from the standard "sublattice" picture of the AFM arise only in a small vicinity (with the size $r < R_c$) of the dislocation line. This size is maximum for the example of the layered AFM given above: in that case, $R_c \sim a\sqrt{J_{\rm ip}/J_{\rm op}}$, where a is the interatomic distance. For typical values of the ratio $J_{\rm op}/J_{\rm ip} \sim 10^{-2}$, we obtain the R_c-value of an order of tens of interatomic distances a [76]. Beyond this region, the local vector $\mathbf{l}$ can be introduced as the difference between the vectors of the spins coupled by the antiferromagnetic interaction. In so doing, we obtain again that, when going along a closed contour drawn through the spin exchange bonds around any dislocation line, the vector $\mathbf{l}$ changes its sign. This result is valid for any dislocation, edge or screw, as well as for any direction of the Burgers vector. A disclination in the AFM can be considered as an antiferromagnetic vortex with a half-integer value of the π_1-topological charge [75].

When going around a dislocation, the sublattices cannot be reconciled, so that the antiferromagnetic vector $\mathbf{l}$ cannot be determined globally. A similar situation with the determination of the displacement vector arises, when developing the theory of elasticity for a crystal with a dislocation. In both cases, the corresponding vector can be determined locally within several overlapping regions of the crystal. In the case of AFMs, the vector $\mathbf{l}$ can be introduced in the regions, where the dislocation line does not pass;

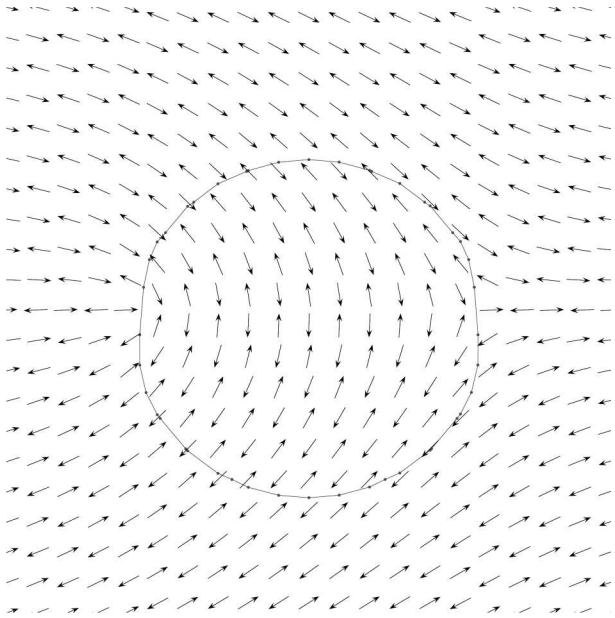

Fig. 1. Distribution of spins in a thin AFM film with two dislocations calculated numerically in the framework of the discrete AFM model with the square lattice [77]. On the closed line, the deviation angles of spins from the direction that they have far from the dislocations equal $\pi/4$

then, the sublattices can be reconciled at the interfaces of the regions. In each of those regions, one can define the vector $\mathbf{l}$ as a single-valued coordinate function $\mathbf{l} = \mathbf{l}(\mathbf{r})$ and use a standard phenomenological approach based on taking the system energy as a functional of the vector $\mathbf{l}$ (the sigma model approach). Afterward, the solutions determined in various regions can be reconciled. For this purpose, it is enough to cut an arbitrary surface ending at the dislocation line and stipulate that the directions of the antiferromagnetic vectors $\mathbf{l}_+$ and $\mathbf{l}_-$ on the different sides of the cut have to be opposite at every surface point or, in the invariant form, $\mathbf{l}_+ \cdot \mathbf{l}_- = -1$. If there are several dislocations, it is necessary to select several such surfaces, one for each dislocation line. Then the cut surfaces will end either at the dislocation line or the AFM surface. In the case of a closed dislocation loop, it is enough to assume that the vector $\mathbf{l}$ has a jump at the end surface that is tightened on the dislocation line (see Figs. 1 and 2).

If the magnetic anisotropy is present, the dislocation can result in the appearance of either a domain wall ending at the dislocation line or several such walls. For a uniaxial AFM with the easy-axis

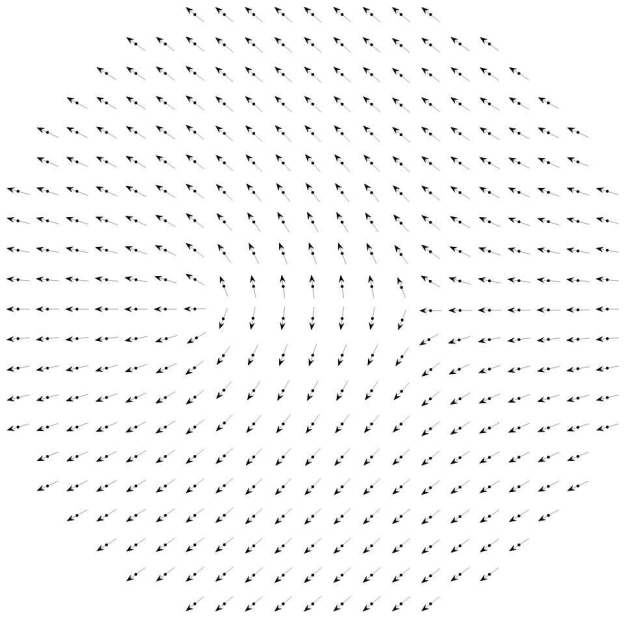

Fig. 2. Distribution of the vector **l** for the system presented in Fig. 1 (an AFM with two dislocations). The cutting line is a linear segment connecting the dislocation location points

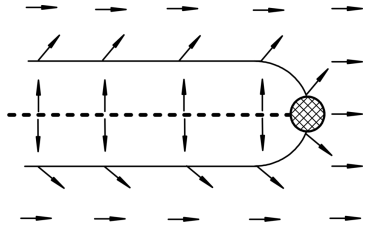

Fig. 3. Schematic diagram for the distribution of the vector **l** near the domain wall in an AFM with the "easy-axis" anisotropy. Here and at the figures below, hatched circles denote singularity regions in the dislocation vicinity, and thick dashed lines mark cutting lines

anisotropy and an AFM with the uniaxial anisotropy in the basis plane, there a 180°-wall ending at the dislocation line emerges (see Figs. 3 and 4). It is clear that a domain structure of the ordinary type, where different domains are separated by domain walls, cannot exist in this case.

However, if there is the fourth-order anisotropy (the principal axis C_4) or the sixth-order anisotropy (the principal axis C_3 or C_6) in the basal plane of the uniaxial AFM with the anisotropy of the "easy-plane" type, a specific "topological" domain structure becomes possible, where domains are separated by domain walls. When describing this structure, it is

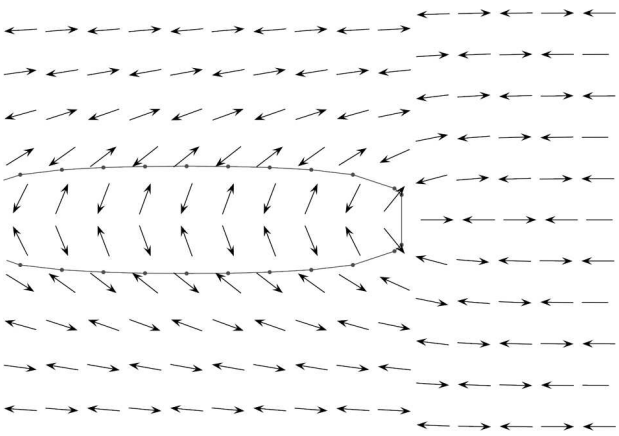

Fig. 4. Spin distribution near a domain wall in an AFM with the easy-axis anisotropy calculated numerically in the framework of the discrete AFM model [77]

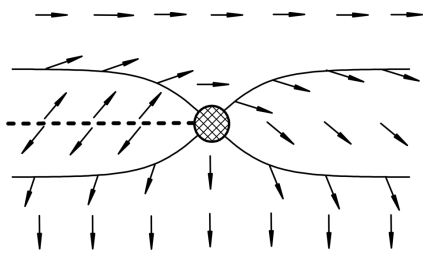

Fig. 5. Schematic diagram for the distribution of the vector **l** in an AFM with the fourth-order anisotropy, which contains a dislocation and a domain wall. The latter has a complicated structure and separates two domains. See further explanations in the text

convenient to assume that the discontinuity interface is "hidden" inside one of those walls. Then, for an AFM with the axis C_4 and a dislocation, there is a structure of two domains with the orthogonal directions of the vector **l**, which are separated by a 90°-wall with a complicated internal structure (see Fig. 5) [73, 74]. For an AFM with the sixth-order anisotropy, the appearance of a structure consisting of three domains separated by 60°-walls can be expected, where the directions of the vector **l** in the domains are oriented at an angle of 60° with respect to each other. A "deficiency" of the turn angle is compensated by the presence of a line that is equivalent to an additional turn of the vector **l** by 180°.

The geometry of topological domain structures is different from that of "standard" domains induced by the dipole or magnetoelastic interaction [71, 72]. For magnets with the fourth-order anisotropy, the classi-

cal Landau structure with four domains is known. For a magnet with the sixth-order anisotropy, one may expect a structure with either six 60°-walls or three 120°-walls (see Fig. 13 in work [72]). For "standard" domains, the role of dislocations is in essence the same as for other (non-topological) defects. Their influence is reduced to a local change in the character of the magnetic anisotropy, so that the inhomogeneous spin state becomes favorable [71,72]. In particular, a structure with three 120°-walls can be stable in the presence of a defect [69].

Let us return to the consideration of AFMs with topological inhomogeneities. Beyond the cuts, the standard AFM theory, which is based on the introduction of sublattices or the vectors $\mathbf{m}$ and $\mathbf{l}$ as single-valued coordinate functions, is applicable. The static energy of the AFM contains a large number of invariants constructed from the components of the vectors $\mathbf{m}$ and $\mathbf{l}$, as well as their gradients. If the states for which $|\mathbf{m}| \sim |\mathbf{l}|$ have to be taken into account – e.g., near the dislocation – the analysis becomes much more complicated, but it can also be carried out in some cases (see works [76, 78–86] and monographs [87, 88]). In the standard Heisenberg AFM far from the dislocation and in a not very strong magnetic field, we may put $|\mathbf{m}| \ll |\mathbf{l}| \simeq 1$ (for details, see work [76]). In this case, we can exclude the vector $\mathbf{m}$ and write the energy in terms of only the vector $\mathbf{l} = \mathbf{L}/|\mathbf{L}| \simeq \mathbf{L}/(2M_0)$, assuming the latter to be a unit one. The phenomenological description of the AFM is carried out on the basis of a single field variable $\mathbf{l} = \mathbf{l}(\mathbf{r}, t)$, with $\mathbf{l}^2 = 1$.

The static energy of the AFM is written as a functional $W[\mathbf{l}]$ of only the vector $\mathbf{l}$ and its gradients. The corresponding expression can be presented in the form

$$W = \int d\mathbf{r} \left[\frac{A}{2} (\nabla \mathbf{l})^2 + w_{\mathrm{a}}(\mathbf{l}) \right], \tag{3}$$

where A is the inhomogeneous exchange constant, $w_{\mathrm{a}}(\mathbf{l})$ the anisotropy energy, and the integration is carried out over the whole magnet volume. The minimization of this energy gives an equilibrium distribution of the vector $\mathbf{l}$. Of course, all constants in all domains, where the vector $\mathbf{l}$ can be determined unambiguously, are identical. It is also evident that if there is an equilibrium state $\mathbf{l}(\mathbf{r})$, then the state $-\mathbf{l}(\mathbf{r})$ is also equilibrium and has the same energy. Hence, it is possible to minimize the energy with regard for the cuts of the type $\mathbf{l} \to -\mathbf{l}(\mathbf{r})$ at the selected special interfaces and obtain a static distribution of the vector $\mathbf{l}$ corresponding to the ground state of the AFM with dislocations. It is clear that the necessity of such cuts makes the AFM state heterogeneous.

The AFM dynamics can be described by a closed equation for $\mathbf{l}$ (it is called the sigma-model equation). The sigma model can be developed in various ways [89–91], which are described in detail in many reviews and books [1,5,6,75,87,91–94] and are not reproduced here. In the simplest case, the sigma-model equation contains the second-order time derivative of $\mathbf{l}$ and looks like

$$\frac{2M_0}{\gamma^2 H_{\mathrm{ex}}} \left(\mathbf{l} \times \frac{\partial^2 \mathbf{l}}{\partial t^2} \right) = A(\mathbf{l} \times \nabla^2 \mathbf{l}) - \left(\mathbf{l} \times \frac{\partial w_{\mathrm{a}}}{\partial \mathbf{l}} \right) + \mathbf{R}, \tag{4}$$

where H_{ex} is the AFM exchange field, γ the gyromagnetic ratio, and the term $\mathbf{R}$ describes the contribution of non-conservative processes – dissipation and spin current (its form will be given below). In the framework of the sigma-model approach, the AFM magnetization $\mathbf{m}$ is a dependent variable, which is expressed in terms of the vector $\mathbf{l}$ and its time derivative. In the most general case,

$$H_{\mathrm{ex}} \mathbf{m} = \frac{1}{\gamma} \left(\frac{\partial \mathbf{l}}{\partial t} \times \mathbf{l} \right) + \mathbf{H}^{(\mathrm{eff})} - \mathbf{l}(\mathbf{H}^{(\mathrm{eff})} \cdot \mathbf{l}), \tag{5}$$

where $\mathbf{H}^{(\mathrm{eff})}$ is an effective field, which includes the external field $\mathbf{H}$ and other symmetry-allowed components depending on the vector $\mathbf{l}$, e.g., the Dzialoshinskii field [94]. For an AFM with the odd translation and in the absence of the external field, $\mathbf{H}^{(\mathrm{eff})} = 0$ and only the first (dynamic) contribution to the magnetization survives. Note that both the dynamic contribution and the contribution of the external field are bilinear in the components of the vector $\mathbf{l}$, so that the magnetization does not change, if its sign changes.

Neglecting the relaxation, the sigma model can be obtained in the framework of the Lagrange formalism. The Lagrange functional is written in the standard form $L = T - W$, where the static energy W [see Eq. (3)] plays the role of a potential energy, and the kinetic energy T is determined by the formula

$$T = \frac{M_0}{\gamma^2 H_{\mathrm{ex}}} \int d\mathbf{r} \left(\frac{\partial \mathbf{l}}{\partial t} \right)^2. \tag{6}$$

The total energy of the dynamic AFM state E is determined as the sum $E = T + W$.

The energy functional (3) has the same form as the standard energy functional for the ferromagnet written in terms of the normalized ferromagnet magnetization $\mathbf{m}_{\rm FM} = \mathbf{M}/M_s$, where M_s is the saturation magnetization. Furthermore, for magnets with similar ions and close values of microscopic parameters (the lattice constant, the exchange integral, and so forth), the values of the parameters entering Eq. (3) will be comparable for AFMs and ferromagnets. However, the spin dynamics is essentially different for those two classes of magnets. The matter is that the Landau–Lifshitz equation for the magnetization,

$$\frac{M_s}{\gamma}\frac{\partial \mathbf{m}_{\rm FM}}{\partial t} = \left(\mathbf{m}_{\rm FM} \times \frac{\delta W[\mathbf{m}_{\rm FM}]}{\delta \mathbf{m}_{\rm FM}}\right),$$

where $W[\mathbf{m}_{\rm FM}]$ is the functional of the energy of the ferromagnet, contains the first-order time derivative. Any term with the first-order time derivative is invariant with respect to the time inversion operation $t \to -t$. Such a term is allowed for ferromagnets, because there is no other symmetry transformation that would change the magnetization sign. However, it is forbidden for the AFM vector $\mathbf{l}$, because it is not invariant with respect to the action of the odd symmetry element of the AFM, which interchanges the sublattices. Therefore, the equation for $\mathbf{l}$ can contain only the second-order time derivative divided by a quantity with the frequency dimensionality. This quantity must be universal and responsible for the AFM ordering. Therefore, the only option for Eq. (4) is the selection of the exchange frequency $\omega_{\rm ex} = \gamma H_{\rm ex}$. A comparison of those two equations taking into account that, first, $M_s = 2M_0$ and, second, the structures of the functionals $W[\mathbf{m}_{\rm FM}]$ and $W[\mathbf{l}]$ are analogous explains the appearance of an additional large parameter (the exchange field) in all dynamic parameters of AFM spin excitations (the exchange enhancement effect).

Thus, the exchange enhancement effects can be directly associated with the peculiarity in the transformation properties of the vector $\mathbf{l}$ and, first of all, with the presence of odd elements of the AFM symmetry group. A purely symmetry-based substantiation of the sigma-model equation was proposed by Andreev and Marchenko [91]. In their approach, the exchange frequency was expressed in terms of a simple physical parameter, the transverse susceptibility of AFM, $\chi_\perp = 2M_0/H_{\rm ex}$.

3. Inhomogeneous Nonlinear Dynamic States of AFMs

If the effective field $\mathbf{H}^{(\rm eff)}$ – in particular, the Dzialoshinskii field – is taken into account, the sigma-model equations become more complicated and include additional components, which are linear in the derivative $\partial\mathbf{l}/\partial t$ (see review [94]). But in our case, i.e. an AFM with the odd translation and in the absence of an external magnetic field, the only possible dynamic term in Eq. (4) is the "inertial" term with $\partial^2\mathbf{l}/\partial t^2$. For uniaxial AFMs with the principal axis $\mathbf{e}$, for which the anisotropy energy depends only on $(\mathbf{e}\cdot\mathbf{l})^2$, this circumstance makes it possible to construct an exact class of dynamic AFM states corresponding to a certain static state $\mathbf{l} = \mathbf{l}_0(\mathbf{r})$. Really, it is easy to verify that a dynamic state of the form of simple precession around the principal AFM axis $\mathbf{e}$ with the frequency ω and satisfies the equation

$$\frac{\partial \mathbf{l}}{\partial t} = \omega\,[\mathbf{e}\times\mathbf{l}] \tag{7}$$

is a solution of the static version of Eq. (4) with the renormalized anisotropy energy $w_{\rm a}(\mathbf{l}) \to \tilde{w}_{\rm a}(\mathbf{l})$, where

$$\tilde{w}_{\rm a} = w_{\rm a} + \omega^2\frac{M_0}{\gamma^2 H_{\rm ex}}\left[(\mathbf{e}\cdot\mathbf{l})^2 - 1\right]. \tag{8}$$

This property of the sigma-model equation was used in this or that form by many authors while analyzing various solitons in AFMs (see the recent works [94–97] and references therein). It allows the construction of dynamic solutions by simply applying formulas (6) and (7) to available static solutions. Naturally, there arise a number of questions at that, in particular, about the physical meaning and stability of the obtained dynamic states. The uniform precession preserves the condition $(\mathbf{l}_+\cdot\mathbf{l}_-) = -1$ along the cut line, because this condition is invariant with respect to rotations. Therefore, transformation (7) can be applied to AFMs with an arbitrary system of dislocations as well.

Now, let us discuss the influence of non-conservative processes: dissipation and the action of a spin current. They are usually described by choosing the term $\mathbf{R}$ in the form

$$\mathbf{R} = \frac{2M_0}{\gamma}\left[-\alpha_G\left(\mathbf{l}\times\frac{\partial\mathbf{l}}{\partial t}\right) + \tau(\mathbf{l}\times(\mathbf{p}\times\mathbf{l}))\right], \tag{9}$$

where the first term, which is proportional to $\partial\mathbf{l}/\partial t$, is a dissipative one in the Gilbert form with the dimensionless constant α_G, and the second one describes

the action of the spin current with the spin polarization directed along the unit vector $\mathbf{p}$. The value of the constant τ is proportional to the pumping current density j, $\tau = \sigma j$, and the specific values of the parameter σ for various device schemes can be found in review [98].

It is easy to verify that Eqs. (7) and (9) are in agreement, if we assume that the vectors $\mathbf{e}$ and $\mathbf{p}$ are parallel to each other, and the precession frequency satisfies the condition

$$\omega = \frac{\tau}{\alpha_G} = j\frac{\sigma}{\alpha_G}. \tag{10}$$

If both conditions are satisfied, we obtain that $\mathbf{R} = 0$, i.e. the action of the spin current compensates the relaxation processes and creates conditions for appearance of steady-state non-uniform precession. The frequency of this precession is proportional to the current magnitude and inversely proportional to the small parameter, the constant α_G. In this regime, the existence of dynamic states is associated only with the overcoming of friction. The estimates made in works [55, 57, 59, 60] showed that, for real AFM parameters and frequencies up to terahertz, the required current density is not high (less than 10^8 A/cm^2), whereas the current densities in already created devices of ferromagnet-based spintronics reach values of up to 10^9 A/cm^2 [51, 99].

For the further analysis, it is convenient to express the unit vector $\mathbf{l}$ in terms of angular variables. Let us choose three orthogonal vectors $(\mathbf{e}, \mathbf{e}_1, \mathbf{e}_2)$ and direct the polar axis along the selected AFM axis $\mathbf{e}$. Then $\mathbf{l}\cdot\mathbf{e} = \cos\theta$, $l_1 = \sin\theta\cos\phi$, and $l_2 = \sin\theta\sin\phi$. The precession state of type (7) is described by the formulae $\theta = \theta(\mathbf{r})$ and $\phi = \omega t$.

The anisotropy energy $w_{\rm a}(\theta)$ for uniaxial magnets is usually selected in the form $w_{\rm a}(\theta) = (K/2)\sin^2\theta$. If $K > 0$, the vector $\mathbf{l}$ in the ground state is directed along the vector $\mathbf{e}$, i.e. the anisotropy of the easy-axis (EA) type is realized. If $K < 0$, then $\mathbf{l}\cdot\mathbf{e} = 0$ in the ground state, i.e. the anisotropy of the easy-plane (EP) type takes place. Taking the explicit expression for $w_{\rm a}(\theta)$ into account, the renormalized anisotropy energy (8) can be written in the form

$$\tilde{w}_{\rm a} = \frac{\tilde{K}}{2}\sin^2\theta, \tag{11a}$$

where

$$\tilde{K} = K - \omega^2\frac{2M_0}{\gamma\omega_{\rm ex}}. \tag{11b}$$

It is easy to see that, in the case of EP AFM, the precession does not change the character of this anisotropy and, if $K < 0$, the quantity $\tilde{K}$ remains negative ($\tilde{K} < 0$) at all frequencies. In the case of EA AFM, the situation is different: the constant $\tilde{K}$ changes its sign at $\omega > \omega_0$, where the frequency $\omega_0 = \sqrt{\omega_{\rm a}\omega_{\rm ex}}$ coincides with the AFM resonance frequency. Here, $\omega_{\rm ex} = \gamma H_{\rm ex}$ is the exchange frequency, $\omega_{\rm a} = \gamma H_{\rm a}$, the anisotropy field $H_{\rm a}$ is defined by the formula $2H_{\rm a}M_0 = K$, and the distribution of the vector $\mathbf{l}$ is described by the function $\theta = \theta(\mathbf{r})$ which is a solution of the well-studied "static" equation

$$A\nabla^2\theta = \tilde{K}\sin\theta\cos\theta. \tag{12}$$

In particular, standard domain walls exist at $\tilde{K} > 0$, i.e. at rather high frequencies ranging from zero to ω_0 [95].

The total energy of the dynamic AFM state, $E = T + W$, can be written as a functional of only the variable θ in the following form:

$$E = \int d\mathbf{r}\,\left[\frac{A}{2}(\nabla\theta)^2 + w_{\rm eff}(\theta)\right], \tag{13a}$$

where

$$w_{\rm eff}(\theta) = w_{\rm a}(\theta) + \omega^2\frac{M_0}{\gamma\omega_{\rm ex}}\sin^2\theta. \tag{13b}$$

In other words, the contribution of precession to the AFM energy can be represented as a addition to the anisotropy energy. Note that this addition is positive, i.e. the contributions of the precession to the system energy $w_{\rm eff}(\theta)$ and the function $\tilde{w}_{\rm a}$, which determines the solution structure, have opposite signs [cf. Eqs. (11b) and (13b)].

4. The application of AFM Disclinations in Spintronics

Let us discuss how the inhomogeneous dynamics described above can be used to generate the desired signal in the form of an alternating current. The universal method, which can be applied to all AFMs, is based on the application of two-layer systems "AFM–normal metal". The rotation of the vector $\mathbf{l}$ in the AFM driven by the spin pumping mechanism generates a spin current with the polarization $\mathbf{j}_{\rm sp} \propto \propto (\mathbf{l}\times\partial\mathbf{l}/\partial t)$ in the normal-metal layer (the "reverse" spin current). Owing to the inverse spin Hall effect, this spin current creates an electric current $\mathbf{j}_{\rm ISH}$ in

the metal, which flows along the surface in a direction perpendicular to $\mathbf{j}_{\rm sp}$. Heavy metals with strong spin-orbit interaction, such as platinum (Pt) or tantalum (Ta), for which the spin Hall effect is substantial [49], are chosen for such devices. If the spin current $\mathbf{j}_{\rm sp}$ is alternating, the desired signal is obtained in the form of an alternating electric current (for details, see works [57, 59, 98]). Such systems on the basis of ferromagnets have already been implemented, and their high efficiency has been demonstrated [51–54].

For the dynamic state described above, the polarization of the "reverse" spin current $\mathbf{j}_{\rm sp}$ is determined by the formula

$$\mathbf{j}_{\rm sp} \propto \omega \left[\sin^2\theta \mathbf{e} - \sin\theta\cos\theta \left(\mathbf{e}_1 \cos\omega t + \mathbf{e}_2 \sin\omega t\right)\right]. \tag{14}$$

For all precession amplitudes $\theta \neq 0$, a direct spin current is pumped into the metal substrate, which creates an additional relaxation channel in the system (for more details, see works [59, 100]). At the same time, the alternating current oscillating with the frequency ω emerges only under the condition $\sin\theta\cos\theta \neq 0$. In the case of homogeneous precession in a uniaxial AFM, the angle value is determined from the condition $d\tilde{w}_{\rm a}/d\theta = 0$. In the framework of the standard model (11), $d\tilde{w}_{\rm a}/d\theta \propto \sin\theta\cos\theta$, and the homogeneous precession of the vector $\mathbf{l}$ corresponds to the angle $\theta = \pi/2$, i.e. there is no desired ac signal [59]. In this case, the vector $\mathbf{l}$ rotates idle, so to speak.

The values $\theta \neq \pi/2$ inevitably arise in the case of inhomogeneous states like the domain wall or the spin disclination. Let us discuss the properties of such states and the possibility to use them for creating spintronic generators. While creating nanogenerators, where a ferromagnet particle is excited by a spin-polarized current, the application of two-dimensional solitons such as magnon droplets in thin films with perpendicular anisotropy has considerable advantages over the systems with uniformly magnetized particles [101–103]. A possibility of the nonplanar spin rotation and the alternating current generation due to the presence of regions, where $\theta \neq \pi/2$ [see Eq. (14)], may become an important advantage of inhomogeneous AFM states. A single atomic dislocation creates a nonlocalized inhomogeneous state, a spin disclination. It is generally assumed that a planar state is typical of it, i.e. the spin distribution is inhomogeneous, but the spins lie in the same plane. A simple rotation of the spins in this plane, as well as a homogeneous planar rotation, contributes to the dissipation, but does not create a ac signal.

Let us consider the variants of more complicated dynamic regimes. The most interesting in AFMs, as it was in ferromagnets, are localized solitons. Far from a soliton, the vector $\mathbf{l}$ is parallel to the rotation axis. Such localized spin inhomogeneities, which are similar to magnetic droplet solitons, arise due to the presence of either closed dislocation loops in three-dimensional AFMs or point dislocations in two-dimensional (2D) AFMs [77]. The application of 2D models makes the analysis substantially simpler. In particular, Eqs. (13) are reduced to a static (elliptic) two-dimensional sine-Gordon equation, which is exactly integrable. It has a number of exact solutions that describe different non-uniform states such as vortices, disclinations, and vortex dipoles [77, 104, 105] (see also book [88]). The results obtained while analyzing 2D models can be applied to describe thin AFM films, the thickness of which is less than all characteristic dimensions of the problem, namely, the distance R between dislocations and the exchange length $l_0 = \sqrt{A/K}$, which determines the domain wall thickness. In real AFMs, the exchange length exceeds 10 nm [77]. An investigation of just such films is relevant for their applications in spintronics, because the action of spin current becomes less effective, if the film is thicker than 10 nm. When describing an AFM thin film in the framework of the 2D model, the substitution $\int d\mathbf{r} \to L \int dxdy$, where L is the film thickness, and x and y are the coordinates in the film plane, is implied.

In the framework of the 2D model, the vector $\mathbf{l}$ can be assumed to depend on only two spatial variables, say, $\mathbf{l} = \mathbf{l}(x, y)$. The domain of the function $\mathbf{l}(x, y)$ is a plane with the cut out neighborhood of the singular points containing the dislocations. From those singular points start the cutting lines, at which the vector $\mathbf{l}$ has a discontinuity of the form $\mathbf{l}_{(+)} = -\mathbf{l}_{(-)}$, where $\mathbf{l}_{(+)}$ and $\mathbf{l}_{(-)}$ stand for the directions of the vector $\mathbf{l}$ at different edges of the cut. Those lines either connect the dislocation points or end at the AFM boundary. It is convenient to choose the cutting lines in such a way that their symmetry would correspond to the symmetry of the dislocation system and the AFM anisotropy energy.

Let us restrict the analysis to the simplest case in which localized states are possible, namely, a thin

AFM film with a dislocation pair. To be more specific, let us assume the dislocations to be located on the x-axis at the distance R from the coordinate origin, i.e. their coordinates are $(-R, 0)$ and $(R, 0)$. It is convenient to select the cutting line in the AFM plane as a linear segment connecting the dislocations, as well as the parameters with the values $\theta = \pi/4$ and $y = 0$ (see Fig. 6).

The exact analytic solution of this problem in the static case has the simplest form for the isotropic AFM [77]. Let us discuss it in more details, because it also describes the EA AFM in the most interesting case of high frequencies, $\omega \sim \omega_0$. With our angular parametrization of the vector $\mathbf{l}$, the solution in the upper half-plane $y \geq 0$ looks like

$$\tan 2\theta = \frac{2yR}{x^2 + y^2 - R^2}. \tag{15}$$

To describe $\mathbf{l}$ in the lower half-plane, it is enough to make the substitution $\theta \to -\theta$. Far from the soliton, we have $\theta \to 0$, i.e. $\mathbf{l} \to \mathbf{e}$. The value of $|\theta|$ is maximum on the cutting line $-R < x < R$, namely, $\theta = \pm\pi/2$ (for instance, $\mathbf{l} = \mathbf{e}_1$ at $y \to +0$ and $\mathbf{l} = -\mathbf{e}_1$ at $y \to -0$. The value of the desired signal (alternating current) is maximum for the values $\theta = \pm\pi/4$. One can easily see from solution (15) that this characteristic value is reached on the circle $x^2 + y^2 = R^2$, which passes through the dislocation points. Hence, the region, where the ac signal can be efficiently generated, has a large area of about R^2. The isotropic solution (15) also gives $\theta \to 0$ far from the soliton, so that there is no generation and no losses for the direct current excitation.

A real AFM is always characterized by a certain magnetic anisotropy. For the EA anisotropy, the corresponding analytic solutions (rather cumbersome) were obtained in works [104,105], and they were studied numerically in the framework of the lattice model for the AFM [77]. The analysis showed that if the anisotropy is weak or the disclinations are located close to each other, i.e. if $R < l_0$, solution (15) is valid with a high accuracy. But if the exchange length is comparable to the distance between the dislocations, $2R$, then the region, where spins substantially deviate from the easy axis ($|\theta| \geq \pi/4$), decreases and loses its circular symmetry (see Figs. 3, 4, and 5). In the case $R \gg l_0$, the width of the characteristic region with $|\theta| \sim \pi/4$ measured toward the y-axis becomes x-independent, which means that a spin distribution

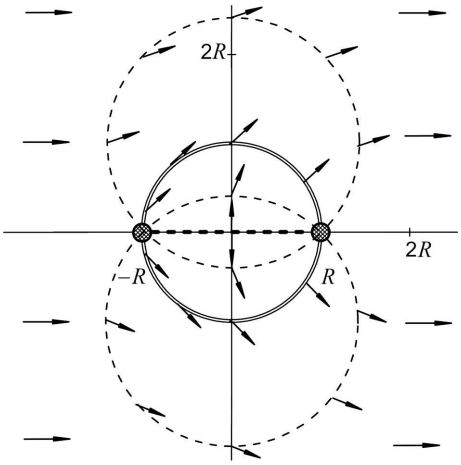

Fig. 6. Distribution of the vector $\mathbf{l}$ in a two-dimensional isotropic AFM obtained from the exact solution of the problem [77]. The circle with a double contour corresponds to the value $\theta = \pi/4$; on the circles with dashed contours, $\theta = 3\pi/8$ (inside the circle with $\theta = \pi/4$) or $\pi/8$ (outside the circle with $\theta = \pi/4$)

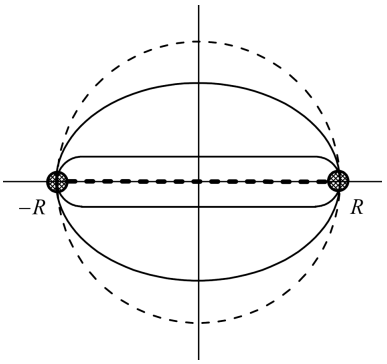

Fig. 7. Shape transformation of the specific curve on which $\theta = \pi/4$, as the anisotropy constant increases

of the same type as in the 180° antiferromagnetic domain wall is formed near the segment connecting the dislocations (see Fig. 7). As a result, the size of the region, where a varying signal can be efficiently generated, diminishes. Its area becomes equal to about $l_0 R$ rather than R^2, as was in the isotropic case.

Now, let us consider how the precession dynamics affects the character of the vector $\mathbf{l}$ distribution. According to formula (11), the effective EA-anisotropy constant decreases at the precession. As a result, the quantity $l_0(\omega) = l_0/\sqrt{1 - \omega^2/\omega_0^2}$, where $\omega_0 = \sqrt{\omega_a \omega_{ex}}$ is the frequency of the linear AFM resonance, increases, as well as the size of the "useful" region, where $|\theta| \sim \pi/4$. In particular, the prob-

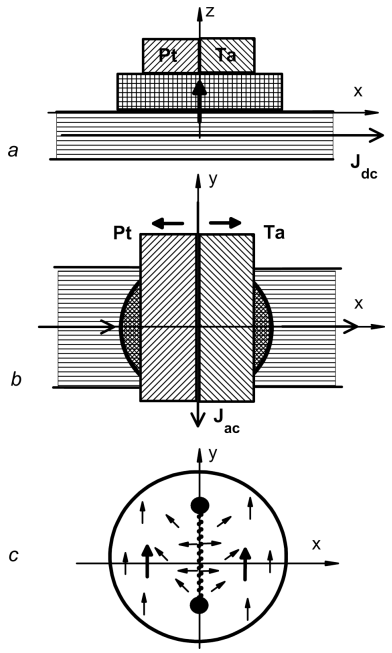

Fig. 8. Schematic diagrams illustrating a microwave generator with a thin film of a uniaxial AFM with two dislocations used as an active element. Panels *a* and *b* demonstrate the device views in the direction of the axes y (the easy axis of the AFM) and z, respectively, and panel *c* presents some details for the active layer in the AFM. Different elements are hatched differently. The open-head arrows indicate the directions of electric current flow: the direct current that creates the spin current in the active element in panel *a* and the alternating signal in panel *b*. The triangle-head thick arrows indicate the directions of the spin current flow: the spin-Hall current in the active element (*a*), and the (antiparallel) currents from the active element in the current-collecting Pt and Ta layers (*b*). In panel *c*, thin arrows indicate the directions of the vector $\mathbf{l}$, and two thick arrows (parallel) the direction of the spin current polarization

lem becomes effectively isotropic, i.e. $l_0(\omega) > R$, at $\omega \geq \omega_0\sqrt{1 - l_0^2/R^2}$ (naturally, there also must be $\omega < \omega_0$) even, if $R \gg l_0$.

While analyzing the spin dynamics, any relative orientation of the "spin" coordinate system (the vectors $\mathbf{e}$, $\mathbf{e}_1$, and $\mathbf{e}_2$) and the xy-plane of the magnet (the unit vectors $\mathbf{e}_x$ and $\mathbf{e}_y$) can be chosen. In real spintronic generators, their orientation is determined by the direction of the polarization vector $\mathbf{p}$ of the spin current that is used to excite the spin dynamics. Note that, in this case, a metal can also play the role of AFM, i.e. not only the spin Hall effect can be used for the pumping but also the standard spin-valve scheme. In the case of the spin Hall effect, the directions of the electric and spin currents and the polarization of the spin current are three mutually orthogonal vectors. However, only the spin Hall effect is suitable for producing the signal, because the standard method based on the giant magnetoresistance effect is not applicable to the "pure" AFM. This means that the polarization direction of the "reverse" spin current $\mathbf{j}_{\rm sp}$ (14) which generates the desired signal must be parallel to the plane of the normal-metal film.

When the pumping is performed making use of the spin Hall effect, the polarization $\mathbf{p}$ is always directed in parallel to the magnet plane. Because of the condition $\mathbf{p} \parallel \mathbf{e}$, the EA AFM must lie in the film plane in this case. This geometry was used in works [49, 50] while studying the spin pumping with the help of AFM. Assuming $\mathbf{e} \parallel \mathbf{e}_x$, we obtain that $\mathbf{e}_1 \parallel \mathbf{e}_y$, $\mathbf{e}_2 \parallel \mathbf{e}_z$, $\mathbf{j}_{\rm sp} \propto \omega \mathbf{e}_y \sin\theta\cos\theta\cos\omega t$, and the alternating electric current, which is directed perpendicularly to $\mathbf{j}_{\rm sp}$, flows in the direction of the x-axis, i.e. in the direction perpendicular to that of the electric current used for the pumping. If the polarization $\mathbf{p}$ of the pumping current and the EA-AFM orientation (the vector $\mathbf{e}$) are directed perpendicularly to the film plane, then the directions of both the current

$$\mathbf{j}_{\rm sp} \propto \omega \sin\theta\cos\theta\,(\mathbf{e}_1\cos\omega t + \mathbf{e}_2\sin\omega t)$$

and the alternating electric current rotate in the film plane.

A common property for all generators, where domain walls or disclinations are used consists in that the value of the quantity $\mathbf{j}_{\rm sp}^{\rm (tot)} = \int \mathbf{j}_{\rm sp} dxdy$ averaged over the specimen equals zero, because the function combination $\sin\theta\cos\theta$ changes its sign at the substitution $y \to -y$. Therefore, the signals have to be read out independently from the film areas, where $\sin\theta\cos\theta \gtrless 0$. In doing so, the signals of the same sign should be summed up. Here, a trick used in work [49] can be applied: two nanowires made of heavy metals with different signs of the spin-Hall angle, i.e. different ratios between the spin and electric currents, should be arranged in parallel to each other. For this purpose, such metals as, e.g., tantalum and platinum can be used [49]. If the wires are in contact with two film areas, where $\mathbf{j}_{\rm sp}$ has different signs, the spin currents induced in them will have opposite directions, but the electric currents will have the same direction, i.e. the effect is obtained, if the wires are simply connected in parallel (see Fig. 8).

It is worth noting a scheme, where disclinations in an AFM with the EA-type anisotropy are used, and which demonstrates a useful feature in the real case $R \gg l_0$. At low current values, the precession frequency is small. Also small (of an order of $l_0 R$) is the area of the region that produces the desired signal. But the same region also contributes to the dissipation associated with the direct current pumping. Therefore, this additional dissipation is also low. As the current increases, the frequency grows, together with the size of the "useful" system region, where $\theta \sim \pi/4$ (up to R^2 at $\omega \to \omega_0$). Hence, the amplitude of the desired signal increases with its frequency. This is a unique property of all schemes of "purely spintronic" nanogenerators, in which the spin-current effects are used both to excite spin oscillations in the AFM and to obtain the desired signal.

5. Conclusions

Thus, even in the presence of atomic dislocations and singularities generated by them (spin disclinations), the spin dynamics of antiferromagnets can be described on the basis of the standard sigma-model equation for an antiferromagnetic unit vector **l**. The presence of spin disclinations leads to the appearance of dynamic states, which correspond to the inhomogeneous spatial precession of the spins. Such an internal dynamics of spin disclinations and related domain walls can be useful for the creation of a spin-Hall nanogenerator with spin-current pumping, which is characterized by a low excitation threshold. Hence, atomic defects (dislocations) and spin defects (disclinations and domain walls) may be useful for the creation of spintronic devices.

Note that the presence of dislocations is an inherent property of real crystals, in particular, thin single-crystalline films obtained by the epitaxy methods and used in spintronics. The analysis of the role of dislocations and other defects in nano-sized magnetic specimens used in spintronics and, especially, probable useful properties of such defects, is just getting started. Note the recent work [106], where it was shown that screw dislocations can enhance the effective spin-orbit interaction in semiconductors. A possibility to stabilize and even amplify the spin current in magnets with a screw dislocation was also mantioned [107].

It is also worth noting that the role of dislocations in AFMs is not limited to the creation of singular distributions for the vector **l**. Domain walls in AFMs with a weak anisotropy in the basis plane can be stabilized by means of the so-called "metallurgical defects" [72]. The latter distort the crystal lattice and locally change the directions of anisotropy fields. In this case, a "normal" domain wall can exist far from the defect, and, being a spin inhomogeneity with a fixed size, it can also be used to create a spin-Hall nanogenerator.

1. E.A. Turov, A.V. Kolchanov, V.V. Menshenin, I.F. Mirsaev, and V.V. Nikolaev, *Symmetry and Physical Properties of Antiferromagnets* (Fizmatlit, 2001) (in Russian).
2. A.G. Gurevich. *Magnetic Resonance in Ferrites and Antiferromagnets* (Nauka, 1973) (in Russian).
3. K.P. Belov, A.K. Zvezdin, A.M. Kadomtseva, R.Z. Levitin. *Orientational Transitions in Rare-Earth Magnets* (Nauka, 1979) (in Russian).
4. B.A. Ivanov. Ultrafast spin dynamics and spintronics for ferrimagnets close to the spin compensation point (Review). *Low Temp. Phys.* **45**, 935 (2019).
5. V.G. Bar'yakhtar, B.A. Ivanov, M.V. Chetkin. Dynamics of domain walls in weak ferromagnets. *Usp. Fiz. Nauk* **146**, 417 (1985) [*Sov. Phys. Uspekhi* **28** (7), 563 (1985)].
6. V.G. Bar'yakhtar, M.V. Chetkin, B.A. Ivanov, S.N. Gadetskii. *Dynamics of Topological Magnetic Solitons. Experiment and Theory.* Tracts in Modern Physics **129** (Springer, 1994).
7. A. Kirilyuk, A.V. Kimel, Th. Rasing. Ultrafast optical manipulation of magnetic order. *Rev. Mod. Phys.* **82**, 2731 (2010).
8. B.A. Ivanov. Spin dynamics of antiferromagnets under action of femtosecond laser pulses (Review article). *Low Temp. Phys.* **40**, 91 (2014).
9. V.V. Eremenko, N.F. Kharchenko, Yu.G. Litvinenko, V.M. Naumenko. *Magneto-Optics and Spectroscopy of Antiferromagnets* (Naukova Dumka, 1989) (in Russian).
10. E.A. Turov. *Kinetic, Optical, and Acoustic Properties of Antiferromagnets* (Urals Branch of the Russian Academy of Sciences, 1990) (in Russian).
11. G.S. Krinchik, M.V. Chetkin. Transparent ferromagnets. *Sov. Phys. Usp.* **12**, 307 (1969).
12. G.A. Smolenskii, R.V.Pisarev, I.G. Sinii. Birefringence of light in magnetically ordered crystals. *Sov. Phys. Usp.* **18**, 410 (1975).
13. A.K. Zvezdin, V.A. Kotov. *Modern Magnetooptics and Magnetooptical Materials* (Institute of Physics, Bristol, 1997).
14. A.S. Borovik-Romanov, N.M. Kreines. Brillouin–Mandelstam scattering from thermal and excited magnons. *Phys. Rep.* **81**, 351 (1982).
15. E.A. Turov, V.G. Shavrov. Broken symmetry and magnetoacoustic effects in ferroand antiferromagnetics. *Sov. Phys. Usp.* **26**, 593 (1983).
16. I.E. Dzialoshinskii. Thermodynamical theory of "weak" ferromagnetism in antiferromagnetic substances. *Sov. Phys. JETP* **5**, 1259 (1957).

17. I.E. Dzialoshinskii. The magnetic structure of fluorides of the transition metals. *Sov. Phys. JETP* **6**, 1120 (1958).
18. S.S. Dhillon, M.S. Vitiello, E.H. Linfield, A.G. Davies, M.C. Hoffmann, J. Booske, C. Paoloni, M. Gensch, P. Weightman, G.P. Williams, E. Castro-Camus, D.R.S. Cumming *et al.* The 2017 terahertz science and technology roadmap. *J. Phys. D: Appl. Phys.* **50**, 043001 (2017).
19. A.V. Kimel, A. Kirilyuk, A. Tsvetkov, R.V. Pisarev, Th. Rasing. Laser-induced ultrafast spin reorientation in the antiferromagnet $TmFeO_3$. *Nature* **429**, 850 (2004).
20. A.V. Kimel, A. Kirilyuk, P.A. Usachev, R.V. Pisarev, A.M. Balbashov, Th. Rasing. Ultrafast non-thermal control of magnetization by instantaneous photomagnetic pulses. *Nature* **435**, 655 (2005).
21. A.M. Kalashnikova, A.V. Kimel, R.V. Pisarev, V.N. Gridnev, A. Kirilyuk, Th. Rasing. Impulsive generation of coherent magnons by linearly polarized light in the easy-plane antiferromagnet $FeBO_3$. *Phys. Rev. Lett.* **99**, 167205 (2007).
22. A.M. Kalashnikova, A.V. Kimel, R.V. Pisarev, V.N. Gridnev, P.A. Usachev, A. Kirilyuk, Th. Rasing. Impulsive excitation of coherent magnons and phonons by subpicosecond laser pulses in the weak ferromagnet $FeBO_3$. *Phys. Rev. B* **78**, 104301 (2008).
23. T. Satoh, S.-J. Cho, R. Iida, T. Shimura, K. Kuroda, H. Ueda, Y. Ueda, B.A. Ivanov, F. Nori, M. Fiebig. Spin oscillations in antiferromagnetic NiO triggered by circularly polarized light. *Phys. Rev. Lett.* **105**, 077402 (2010).
24. T. Satoh, R. Iida, T. Higuchi, Y. Fujii, A. Koreeda, H. Ueda, T. Shimura, K. Kuroda, V.I. Butrim, B.A. Ivanov. Excitation of coupled spin–orbit dynamics in cobalt oxide by femtosecond laser pulses. *Nat. Commun.* **8**, 638 (2017).
25. C. Tzschaschel, K. Otani, R. Iida, T. Shimura, H. Ueda, S. Günther, M. Fiebig, T. Satoh. Ultrafast optical excitation of coherent magnons in antiferromagnetic NiO. *Phys. Rev. B* **95**, 174407 (2017).
26. T. Satoh, R. Iida, T. Higuchi, M. Fiebig, T. Shimura. Writing and reading of an arbitrary optical polarization state in an antiferromagnet. *Nat. Photon.* **9**, 25 (2014).
27. C. Tzschaschel, T. Satoh, M. Fiebig. Tracking the ultrafast motion of an antiferromagnetic order parameter. *Nat. Commun.* **10**, 3995 (2019).
28. J. Nishitani, K. Kozuki, T. Nagashima, M. Hangyo. Terahertz radiation from coherent antiferromagnetic magnons excited by femtosecond laser pulses. *Appl. Phys. Lett.* **96**, 221906 (2010).
29. T. Higuchi, N. Kanda, H. Tamaru, M. Kuwata-Gonokami. Selection rules for light-induced magnetization of a crystal with threefold symmetry: The case of antiferromagnetic NiO. *Phys. Rev. Lett.* **106**, 047401 (2011).
30. J. Nishitani, T. Nagashima, M. Hangyo. Coherent control of terahertz radiation from antiferromagnetic magnons in NiO excited by optical laser pulses. *Phys. Rev. B* **85**, 174439 (2012).
31. A.V. Kimel, B.A. Ivanov, R.V. Pisarev, P.A. Usachev, A. Kirilyuk, Th. Rasing. Inertia-driven spin switching in antiferromagnets. *Nat. Phys.* **5**, 727 (2009).
32. D. Afanasiev, B.A. Ivanov, A. Kirilyuk, Th. Rasing, R.V. Pisarev, A.V. Kimel. Control of the ultrafast photoinduced magnetization across the Morin transition in $DyFeO_3$.*Phys. Rev. Lett.* **116**, 097401 (2016).
33. H.V. Gomonay, V.M. Loktev. Spin transfer and current-induced switching in antiferromagnets. *Phys. Rev. B* **81**, 144427 (2010).
34. E.V. Gomonay V.M. Loktev. Spintronics of antiferromagnetic systems (Review article). *Low Temp. Phys.* **40**, 17 (2014).
35. V. Baltz, A. Manchon, M. Tsoi, T. Moriyama, T. Ono, Y. Tserkovnyak. Antiferromagnetic spintronics. *Rev. Mod. Phys.* **90**, 015005 (2018).
36. M.B. Jungfleisch, W. Zhang, A. Hoffmann. Perspectives of antiferromagnetic spintronics. *Phys. Lett. A* **382**, 865 (2018).
37. P.A. Popov, A.R. Safin, A. Kirilyuk, S.A. Nikitov, I. Lisenkov, V. Tyberkevich, A. Slavin. Voltage-controlled anisotropy and current-induced magnetization dynamics in antiferromagnetic-piezoelectric layered heterostructures. *Phys. Rev. Appl.* **13**, 044080 (2020)
38. P. Stremoukhov, A. Safin, A. Kirilyuk. THz generation and frequency manipulation in AFM/HM interfaces. *J. Phys.: Conf. Ser.* **1461**, 012171 (2020).
39. B.I. Halperin, P.C. Hohenberg. Hydrodynamic theory of spin waves. *Phys. Rev.* **188**, 898 (1969).
40. E.B. Sonin. Analogs of superfluid currents for spins and electron-hole pairs. *Sov. Phys. JETP* **47**, 1091 (1978).
41. S. Takei, B. I. Halperin, A. Yacoby, Y. Tserkovnyak. Superfluid spin transport through antiferromagnetic insulators. *Phys. Rev. B* **90**, 094408 (2014).
42. A. Qaiumzadeh, H. Skarsveg, C. Holmqvist, A. Brataas. Spin superfluidity in biaxial antiferromagnetic insulators. *Phys. Rev. Lett.* **118**, 137201 (2017).
43. E.B. Sonin. Spin currents and spin superfluidity. *Adv. Phys.* **59**, 181 (2010).
44. E.B. Sonin. Superfluid spin transport in magnetically ordered solids (Review article). *Low Temp. Phys.* **46**, 436 (2020).
45. R. Khymyn, I. Lisenkov, V.S. Tiberkevich, A.N. Slavin, B.A. Ivanov. Transformation of spin current by antiferromagnetic insulators. *Phys. Rev. B* **93**, 224421 (2016).
46. M. Dabrowski, T. Nakano, D. M. Burn, A. Frisk, D.G. Newman, C. Klewe, Q. Li, M. Yang, P. Shafer, E. Arenholz, T. Hesjedal, G. van der Laan, Z.Q. Qiu, R.J. Hicken. Coherent transfer of spin angular momentum by evanescent spin waves within antiferromagnetic NiO. *Phys. Rev. Lett.* **124**, 217201 (2020).
47. P. Wadley, B. Howells, J. Zelezny, C. Andrews, V. Hills, R.P. Campion, V. Novak, K. Olejnik, F. Maccherozzi, S.S. Dhesi, S.Y. Martin, T. Wagner, J. Wunderlich, F. Freimuth, Y. Mokrousov *et al.* Investigation of magnetic anisotropy and heat dissipation in thin films of compensated antiferromagnet CuMnAs by pump–probe experiment. *Science* **351**, 587 (2016).

48. D. Kriegner, K. Vyborny, K. Olejnik, H. Reichlova, V. Novak, X. Marti, J. Gazquez, V. Saidl, P. Nemec, V.V. Volobuev, G. Springholz, V. Holy, T. Jungwirth. Multiple-stable anisotropic magnetoresistance memory in antiferromagnetic MnTe. *Nat. Commun.* **7**, 11623 (2016).
49. J. Li, C.B. Wilson, R. Cheng, M. Lohmann, M. Kavand, W. Yuan, M. Aldosary, N. Agladze, P. Wei, M.S. Sherwin, J. Shi. Spin current from sub-terahertz-generated antiferromagnetic magnons. *Nature* **578**, 70 (2020).
50. P. Vaidya, S. A. Morley, J. van Tol, Y. Liu, R. Cheng, A. Brataas, D. Lederman, E. del Barco. Subterahertz spin pumping from an insulating antiferromagnet. *Science* **368**, 160 (2020).
51. V.E. Demidov, S. Urazhdin, H. Ulrichs, V. Tiberkevich, A. Slavin, D. Baither, G. Schmitz, S.O. Demokritov. Magnetic nano-oscillator driven by pure spin current. *Nat. Mater.* **11**, 1028 (2012).
52. V.E. Demidov, S. Urazhdin, A. Zholud, A.V. Sadovnikov, S.O. Demokritov. Nanoconstriction-based spin-Hall nano-oscillator. *Appl. Phys. Lett.* **105**, 172410 (2014).
53. Z. Duan, A. Smith, L. Yang, B. Youngblood, J. Lindner, V.E. Demidov, S.O. Demokritov, I.N. Krivorotov. Nanowire spin torque oscillator driven by spin orbit torques. *Nat. Commun.* **5**, 5616 (2014).
54. M. Collet, X. de Milly, O. d'Allivy Kelly, V.V. Naletov, R. Bernard, P. Bortolotti, J. Ben Youssef, V.E. Demidov, S.O. Demokritov, J.L. Prieto, M. Munoz, V. Cros, A. Anane, G. de Loubens, O. Klein. Generation of coherent spin-wave modes in yttrium iron garnet microdiscs by spin-orbit torque. *Nat. Commun.* **7**, 10377 (2016).
55. C.E. Zaspel, E.G. Galkina, B.A. Ivanov. High-frequency current-controlled vortex oscillations in ferrimagnetic disks. *Phys. Rev. Appl.* **12**, 044019 (2019).
56. E.G. Galkina, C.E. Zaspel, B.A. Ivanov, N.E. Kulagin, L.M. Lerman. Limiting velocity and dispersion law of domain walls in ferrimagnets close to the spin compensation point. *JETP Lett.* **110**, 481 (2019).
57. I. Lisenkov, R. Khymyn, J. Akerman, N. X. Sun, B.A. Ivanov. Subterahertz ferrimagnetic spin-transfer torque oscillator. *Phys. Rev. B* **100**, 100409(R) (2019).
58. R. Cheng, D. Xiao, A. Brataas. Terahertz antiferromagnetic spin Hall nano-oscillator. *Phys. Rev. Lett.* **116**, 207603 (2016).
59. R. Khymyn, I. Lisenkov, V. Tyberkevych, B.A. Ivanov, A. Slavin. Antiferromagnetic THz-frequency Josephson-like oscillator driven by spin current. *Sci. Rep.* **7**, 43705 (2017).
60. O.R. Sulymenko, O.V. Prokopenko, V.S. Tiberkevich, A.N. Slavin, B.A. Ivanov, R. Khymyn. Terahertz-frequency spin hall auto-oscillator based on a canted antiferromagnet. *Phys. Rev. Appl.* **8**, 064007 (2017).
61. O. Gomonay, V. Baltz, A. Brataas, Y. Tserkovnyak. Antiferromagnetic spin textures and dynamics. *Nat. Phys.* **14**, 213 (2018).
62. V. Puliafito, R. Khymyn, M. Carpentieri, B. Azzerboni, V. Tiberkevich, A. Slavin, G. Finocchio. Micromagnetic modeling of terahertz oscillations in an antiferromagnetic material driven by the spin Hall effect. *Phys. Rev. B* **99**, 024405 (2019).
63. R.E. Troncoso, K. Rode, P. Stamenov, J.M.D. Coey, A. Brataas. Antiferromagnetic single-layer spin-orbit torque oscillators. *Phys. Rev. B* **99**, 054433 (2019).
64. R. Khymyn, E. Galkina, B. Ivanov, J. Akerman. Spin-torque nano-oscillator based on magnetic textures in antiferromagnets. In: *Abstracts of the International conference "Nanomagnetism and spintronics – Sol-SkyMag 2018" (San Sebastian, Spain, June 18–22, 2018)*, p. XXX.
65. A.F. Andreev. Strictive superstructures in two-dimensional phase transitions. *JETP Lett.* **32**, 640 (1980).
66. Y.I. Bespyatykh, I.E. Dikshtein, V.V. Tarasenko. Nonuniform magnetoelastic states in ferromagnetic plates in the region of second-order orientational phase transitions. *Fiz. Tverd. Tela* **23**, 3013 (1981) (in Russian).
67. E.V. Gomonai, V.M. Loktev. On the theory of equilibrium magnetoelastic domain structure in easy-plane antiferromagnet. *Fiz. Nizk. Temp.* **25**, 699 (1999) (in Russian).
68. H. Gomonay, V. Loktev. Magnetostriction and magnetoelastic domains in antiferromagnets. *J. Phys. C* **14**, 3959 (2002).
69. V.M. Kalita, A.F. Lozenko. On the magnetoelastic nature of antiferromagnetic domains in easy-plane crystals of iron-group dihalides. *Fiz. Nizk. Temp.* **27**, 489 (2001) (in Russian).
70. V.M. Kalita, A.F. Lozenko, S.M. Ryabchenko, P.A. Trotsenko. Magneto-elasticity and domain structure in antiferromagnetic crystals of iron-group dihalides. *Ukr. Fiz. Zh.* **43**, 1469 (1998) (in Russian).
71. V.M. Kalita, A.F. Lozenko, S.M. Ryabchenko, P.A. Trotsenko. Role of defects in the formation of the multidomain state of easy-plane antiferromagnets with magneto-elastic interaction. *Zh. Èksp. Teor. Fiz.* **126**, 1209 (2004) (in Russian).
72. V.M. Kalita, A.F. Lozenko, S.M. Ryabchenko, P.A. Trotsenko. Magneto-elasticity and domain structure in antiferromagnetic crystals of iron-group dihalides. *Fiz. Nizk. Temp.* **31**, 1042 (2005) (in Russian).
73. I.E. Dzhyaloshinskii. Domains and dislocations in antiferromagnets. *JETP Lett.* **25**, 110 (1977).
74. A.S. Kovalev, A.M. Kosevich. Dislocations and domains in antiferromagnets. *Low Temp. Phys.* **3**, 117 (1977).
75. B.A. Ivanov. Mesoscopic antiferromagnets: statics, dynamics, and quantum tunneling (Review). *Low Temp. Phys.* **31**, 635 (2005).
76. B.A. Ivanov, V.E. Kireev. Spin disclination in a layered antiferromagnet with a screw dislocation. *JETP Lett.* **73**, 188 (2001).
77. V.E. Kireev, B.A. Ivanov. Localized magnetic nonuniformities in an antiferromagnet with a system of dislocations. *Low Temp. Phys.* **45**, 1256 (2019).
78. A.K. Zvezdin. Dynamics of domain walls in weak ferromagnets. *JETP Lett.* **29**, 553 (1979).

79. V.M. Eleonskii, N.N. Kirova, N.E. Kulagin. Accidental degeneracy of self-localized solutions of the Landau–Lifshitz equations. *Zh. Eksp. Teor. Fiz.* **75**, 2210 (1978) (in Russian).
80. V.M. Yeleonsky, N.N. Kirova, N.E. Kulagin. Models of 2-sublattice magnets which can be solved exactly. *Zh. Eksp. Teor. Fiz.* **80**, 357 (1981) (in Russian).
81. V.M. Yeleonsky, N.E. Kulagin. Some novel cases of the integrability of Landau–Lifshitz equations. *Zh. Eksp. Teor. Fiz.* **84**, 616 (1983) (in Russian).
82. V.M. Yeleonsky, N.E. Kulagin. Integrable models in the problem for particle motion in a two-dimensional potential well. *Zh. Eksp. Teor. Fiz.* **85**, 1437 (1983) (in Russian).
83. E.G. Galkina, B.A. Ivanov. Quantum tunneling in a magnetic vortex in a 2D easy-plane magnetic material. *JETP Lett.* **61**, 511 (1995).
84. O.K. Dudko, A.S. Kovalev. Magnetic ordering at the stepped ferro/antiferromagnetic interface. *Low Temp. Phys.* **24**, 422 (1998).
85. O.K. Dudko, A.S. Kovalev. Influence of dislocations on the magnetic structure of two-dimensional anisotropic antiferromagnets. *Low Temp. Phys.* **26**, 603 (2000).
86. E.G. Galkina, A.Yu. Galkin, B.A. Ivanov. Solitons in isotropic antiferromagnets: Beyond the sigma model. *Low Temp. Phys.* **34**, 522 (2008).
87. A.M. Kosevich, B.A. Ivanov, A.S. Kovalev. *Nonlinear Magnetization Waves. Dynamic and Topological Solitons* (Naukova Dumka, 1983) (in Russian).
88. A.B. Borisov, V.V. Kiselev. *Nonlinear Waves, Solitons, and Localized Structures in Magnets.* In 2 vols (Urals Branch of the Russian Academy of Sciences, 2009) (in Russian).
89. I.V. Bar'yakhtar, B.A. Ivanov. Nonlinear magnetization waves in the antiferromagnet. *Sov. J. Low Temp. Phys.* **5**, 361 (1979).
90. H.-J. Mikeska. Non-linear dynamics of classical one-dimensional antiferromagnets. *J. Phys. C* **13**, 2913 (1980).
91. A.F. Andreev, V.I. Marchenko. Symmetry and the macroscopic dynamics of magnetic materials. *Usp. Fiz. Nauk* **130**, 39 (1980) (in Russian).
92. B.A. Ivanov, A.K. Kolezhuk. Solitons in low-dimensional antiferromagnets. *Fiz. Nizk. Temp.* **21**, 355 (1995) (in Russian).
93. H.-J. Mikeska, M. Steiner. Solitary excitations in one-dimensional magnets. *Adv. Phys.* **40**, 191 (1991).
94. E.G. Galkina, B.A. Ivanov. Dynamic solitons in antiferromagnets (Review article). *Low Temp. Phys.* **44**, 618 (2018).
95. E.G. Galkina, R.V. Ovcharov, B.A. Ivanov. Precessional one-dimensional solitons in antiferromagnets with low dynamic symmetry. *Low Temp. Phys.* **43**, 1283 (2017).
96. O.Y. Gorobets, Y.I. Gorobets. 3D analytical model of skyrmion-like structures in an antiferromagnet with DMI. *J. Magn. Magn. Mater.* **507**, 166800 (2020).
97. B.A. Ivanov. Spin dynamics of antiferromagnets and ultrafast spintronics. *J. Exp. Theor. Phys.* **131**, 95 (2020).
98. A. Slavin. V. Tiberkevich. Nonlinear auto-oscillator theory of microwave generation by spin-polarized current. *IEEE Trans. Magn.* **45**, 1875 (2009).
99. S. Bonetti, P. Muduli, F. Mancoff, J. Akerman. Spin-torque oscillator linewidth narrowing under current modulation. *Appl. Phys. Lett.* **94**, 102507 (2009).
100. Y. Tserkovnyak, A. Brataas, G.E.W. Bauer. Enhanced Gilbert damping in thin ferromagnetic films. *Phys. Rev. Lett.* **88**, 117601 (2002).
101. M.A. Hoefer, M. Sommacal, T.J. Silva. Propagation and control of nanoscale magnetic-droplet solitons. *Phys. Rev. B* **85**, 214433 (2012).
102. M. Mohseni, S.R. Sani, J. Persson, T.N.A. Nguyen, S. Chung, Y. Pogoryelov, P.K. Muduli, E. Iacocca, A. Eklund, R.K. Dumas, S. Bonetti, A. Deac, M.A. Hoefer, J. Akerman. Spin transfer torque generated magnetic droplet solitons (invited). *Science* **339**, 1295 (2013).
103. Y. Zhou, E. Iacocca, A.A. Awad, R.K. Dumas, F.C. Zhang, H.B. Braun, J. Akerman. Dynamically stabilized magnetic skyrmions. *Nat. Commun.* **6**, 8193 (2015).
104. A.B. Borisov, S.N. Ionov. Vortices and vortex dipoles in 2D sine-Gordon model. *Physica D* **99**, **18** (1996).
105. A.B. Borisov, V.V. Kiseliev. Vortex dipoles on a soliton lattice background: Solution of the boundary-value problem by inverse spectral transform. *Physica D* **111**, 96 (1998).
106. L. Hu, H. Huang, Z. Wang, W. Jiang, X. Ni, Y. Zhou, V. Zielasek, M.G. Lagally, B. Huang, F. Liu. Ubiquitous spin-orbit coupling in a screw dislocation with high spin coherency. *Phys. Rev. Lett.* **121**, 066401 (2018).
107. O. Gomonay. Crystals with defects may be good for spintronics. *Physics* **11**, 78 (2018).

Received 12.07.20.

Translated from Ukrainian by O.I. Voitenko

О.Г. Галкіна, В.Є. Кіреєв,
Р.В. Овчаров, Р.С. Химин, Б.О. Іванов

СПІНОВА ДИНАМІКА
В АНТИФЕРОМАГНЕТИКАХ З ДОМЕННИМИ
СТІНКАМИ І ДИСКЛІНАЦІЯМИ

Р е з ю м е

Обговорюється спінова динаміка антиферомагнетиків при наявності атомних дислокацій і породжуваних ними спінових дисклінацій. Показано, як звичайне рівняння сигма-моделі може бути використано для опису такої динаміки. Досліджено динамічні стани, яким відповідає неоднорідна в просторі прецесія спінів. Показано, що така внутрішня динаміка спінових дисклінацій і пов'язаних з ними доменних стінок може бути корисною для створення спін-холлівського наногенератора з накачуванням спіновим струмом, що має малий поріг збудження.